Check for updates

Heavy Metal Distribution, Sources and Contamination Assessment in Polluted Marine Sediments: Keratsini Outfall Sewer Area, Saronikos Gulf, Greece

Anastasia Gkaragkouni · Spyros Sergiou · Maria Geraga ·
Helen Papaefthymiou · Dimitrios Christodoulou · George Papatheodorou

Abstract The central sewer of Athens had been discharging untreated sewage from 1950 until 1995 in the marine area between the island of Psyttalia and Keratsini. As a result, a surficial layer of organic mud was formed covering the seafloor. To assess the spatial and temporal distribution of metal contaminants in the area, six sediment cores were collected and analyzed for grain composition, organic carbon content (Corg), and metal concentrations. ICP-MS and AAS were used to determine the following metal concentrations: Cu, Zn, Mo, Ag, Cd, Cr, Pb, Ni, Fe, As, Mn, and Co. Four different lithofacies were identified based on grain size and macroscopic observations. The contamination of the sediments was assessed according to Enrichment factor (EF), Geo-accumulation Index (I_{geo}), and Pollution Loading Index (PLI), the latter was used in order to assess the overall toxicity status of the sediments. Factor analysis was also performed in the heavy metal, Corg, and Ca datasets. R-mode factor analysis indicates at least three different pollution sources in the area, while Q-mode analysis indicates three different groups of sediment samples according to their pollution degree. The present work stands among others to contribute to the better knowledge of the environmental impact of urban wastes on the shallow marine sediments adjoining large cities areas.

Keywords Heavy metals · Environmental pollution · Sewage · Saronikos Gulf · Psyttalia

Highlights
● An organic mud layer lies at Keratsini strait, attributed to the central sewer of Athens
● There is considerable contamination in the organic mud layer covering the sea floor
● The assessment of contamination was based on environmental indices (EF, Igeo, PLI)
● R-mode factor analysis indicates at least three pollution sources

A. Gkaragkouni · S. Sergiou · M. Geraga ·
D. Christodoulou · G. Papatheodorou (✉)
Laboratory of Marine Geology and Physical
Oceanography, Department of Geology, University
of Patras, 26500 Patras, Greece
e-mail: gpapathe@upatras.gr

H. Papaefthymiou
Department of Chemistry, University of Patras,
26500 Patras, Greece

1 Introduction

Heavy metals are of high environmental significance. In small concentrations, they are necessary for the organisms' development, but if they exceed specific concentration limits, they have negative effects on health and they may cause even death (Salomons & Forstner, 1984; Tham et al., 2021). Due to their chemical properties and behavior, metals participate

in various biogeochemical cycles (e.g. water, sulphur, etc.) (Lee et al., 2006; Bhuiyan et al., 2018; Ali et al., 2019). They have good mobility and can be bio-accumulated by marine organisms such as planktic or benthic foraminifera (Samir & El-Din, 2001), algae and plants (Tranchina et al., 2004), and therefore bio-magnify up the food chain with the top predators receiving the largest dose of conservative substances (Clark, 2001; Tranchina et al., 2008), sometimes with damage effects for human beings (i.e. Hg poisoning in Minamata disease (Sindermann, 2006; Tranchina et al., 2008)).

Heavy metals enter marine sediments by two means: natural processes (including erosion of ore-bearing rocks, windblown dust, volcanic activity and forest fires); and processes derived from human activities such as atmospheric deposition, rivers, and direct discharges or dumping (Clark, 2001; Rezaee et al., 2011). Coastal environments have been subjected to significant environmental pollution due to nearby urban activities (Chester & Voutsinou, 1981; Maata & Singh, 2008). Inappropriate and illegal disposal of industrial and urban wastes, agricultural waste, and metal treatment disposals can result in severe environmental problems such as contamination of receiving waterways and associated sediments by heavy metals.

Marine sediments are usually considered the final repository of a wide range of contaminants (Birch & Taylor, 1999; Galanopoulou et al., 2005; Gibert et al., 2009). When heavy metals are released into the water column, they may be transferred rapidly to the sediment texture by adsorption onto suspended particulate matter, followed by sedimentation. The distribution of heavy metals varies with grain size and tends to accumulate in the fine (< 63 μm) size fraction of the sediments. In addition, sediments remain in an area for a long period of time providing a reliable pollution indicator for that area (Moore & Reynolds, 1989; Salomons & Forstner, 1984; Tessier, 1982). Consequently, a common feature in the seafloor of coastal environments adjoining large urban areas is the deposition of sludge; a surficial layer of mud enriched in organic components and heavy metals, all associated with wastes disposal. During the 1980s, several studies nearby high populated regions revealed the presence of this surficial organic-rich layer and its relative environmental effects; Oviatt et al. (1987) reported

hypoxic conditions on the seafloor of the New York Bight area while Heap et al. (1991) underlined the need of strict controls on the sludge deposition for the cities of London and Edinburgh. Vertical distribution of metals in sediment cores and profile sections can also act as a historical record of human activities and provide insights on the accumulation of metal contaminants over time (Lepland et al., 2010; Valette-Silver, 1993).

Many authors have focused their attention on sediments from industrialized coastal areas and found that metal concentrations in sediments can be a valuable tool to evaluate the degree of environmental pollution. Among the characteristic examples of coastal regions contaminated from urban waste are Palermo; Gulf in Italy (Tranchina et al., 2008), Victoria harbor in Hong Kong (Tang et al., 2008), Naples harbor in Italy (Sprovieri et al., 2007), Barcelona Harbor in Spain, (Gibert et al., 2009), Asaluyeh Port in Persian Gulf (Delshab et al., 2017), Estuaries in eastern China (Bi et al., 2017), the southern coast of Sfax, Gabe Gulf, Tunisia (Naifar et al., 2018), Thessaloniki Bay, Greece (Christophoridis et al., 2017), and Patras Harbor (Papaefthymiou et al., 2010).

It was also found that multivariate statistics such as factor analysis (R-mode and Q-mode) may be a useful method for assessing interrelations between chemical variables. This method has been successfully applied in sediment geochemistry (Cukrov et al., 2011; Karageorgis et al., 2011; Papatheodorou et al., 1999, 2002; Wang et al., 2011) and hydrochemistry (Lambrakis et al., 2004; Papatheodorou et al., 2006; Voudouris et al., 1997).

The pollution problems in Saronikos gulf arise mainly from the former discharge of about 600,000 m^3/day of untreated wastewater into the northern part of the gulf. This process was ongoing for more than 40 years; from 1950 until 1995. High concentrations of heavy metals have been noted in several studies from the gulf area over the past few decades: Papakostidis et al. (1975) determined concentrations 8–200 higher than those of the bedrock for the following metals Sb, As, Cr, Au, Ag, Hg, Zn. Grimanis et al (1977) determined 17 trace elements in higher concentrations than normal (even 200 higher for As). Additionally, Voutsinou-Taliadouri (1981) determined very high Cu, Fe, Zn Corg concentrations compared to natural sediments. Moreover, Galanopoulou et al.

(2009) determined highly elevated Cd, Pb, W, Zn, As, Se, Cr, Cu, and Corg values. Finally, Papaefthymiou et al. (2017) determined the levels and depth distributions of the natural radionuclides U, Th, Ra, K and artificial Cs by γ-ray spectrometry, while the concentrations of 26 elements were measured by INAA. However, the previous studies in Saronikos gulf did not focus on the area between Keratsini and Psyttalia, where the outfall sewer was located nor used more sophisticated multivariate statistical techniques such as factor analysis.

Therefore, the aim of the present study is (a) to assess heavy metal contamination in sediments between Psyttalia and Keratsini, (b) to investigate and explain the complex relations among many geochemical variables using multivariate statistical methods, (c) to visualize and evaluate temporal changes in the consistency and composition of the contaminated sediments, and (d) to indicate possible anthropogenic sources for certain metals. In this way, the present study contributes to the knowledge of the pollution impact of urban wastes to the coastal and marine environment adjoining large urban areas.

2 Study Area

North Saronikos gulf is a seriously polluted marine environment, especially the area between the island of Psyttalia and Keratsini, where the strait has a width

Fig. 1 Study area and locations of sampling sites (Psyttalia — Keratsini Strait, Saronikos Gulf, Greece). Areas **A–D** derived from the geophysical data are also noted
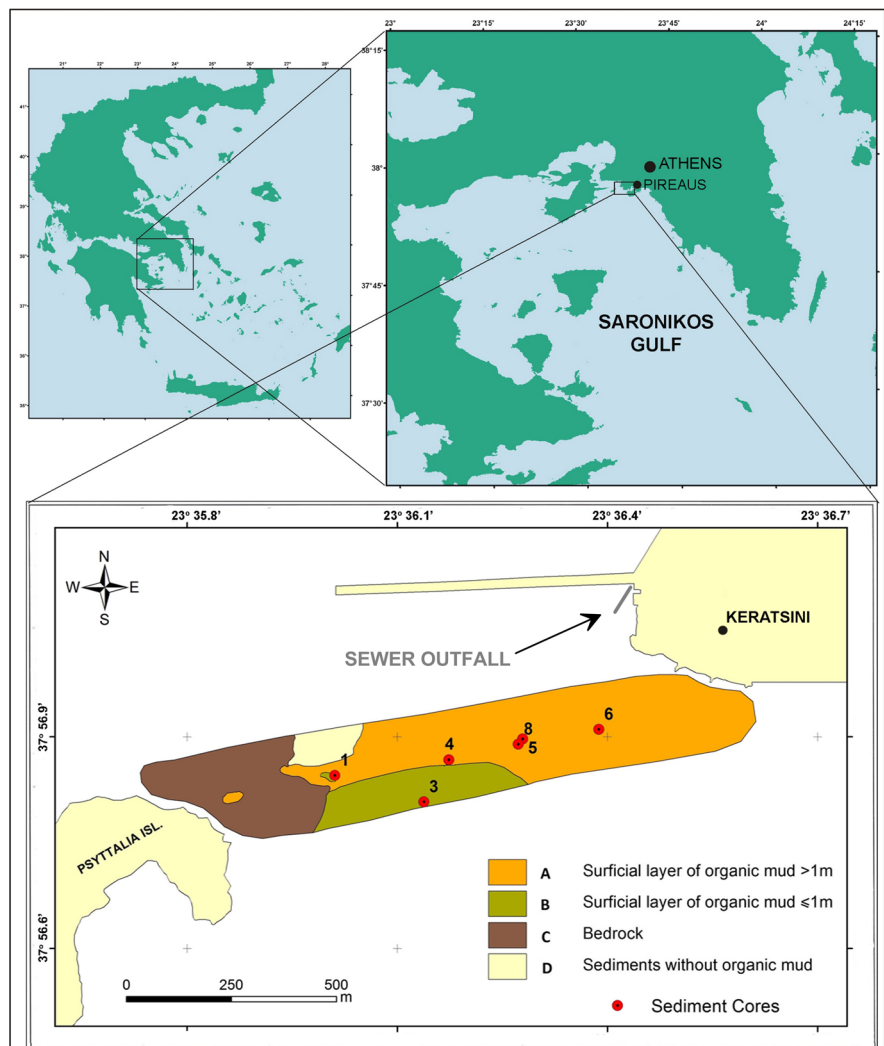
of about 1200 m (Fig. 1). The survey area consists of a narrow strip (1200×200 m) connecting the Psyttalia island with the Keratsini coast (Fig. 1). The broader area of Saronikos Gulf was formed under the influence of tectonic activity during the Quaternary period along with deposition of marine and fluvial sediments (Theodorou & Perissoratis, 1991). The island of Psyttalia consists mostly of Triassic limestones covered with Neogene and Quaternary sediments, while Keratsini consists mostly of marls, sandstones, and conglomerates (Theodorou & Perissoratis, 1991).

For more than four decades, this area had been receiving the urban and a great part of the industrial wastes of the city of Athens through the main sewer. During this period, Athens which is the capital of Greece almost tripled its population; specifically, from 1951 until 1991, the population was multiplied by 2.3 (Kotzamanis, 1997). Additionally, Saronikos gulf receives sewage from the industrial area of Elefsina and the port of Piraeus. The latter, being located in the crossroads of 3 continents; Asia, Europe, and Africa, is the largest commercial port in Greece and among the largest in Europe, while the industrial zone of Athens is settled in the broader area of Elefsina, and Keratsini. Many industries have been located in that area since 1900 and reached their largest number between 1950 and 1990. Among them stand a refinery company, shipyards, Fertilizer Company, an oil mill, and a steel industry. The sewer was built in the 1950s at Keratsini and used to collect the flow of the sewage networks of the area of the capital, carrying urban and some industrial wastes, as well as storm water from areas of the combined network. The total sewage flow discharging to the shallow Keratsini bay was estimated to be about 600,000 m³/day in a depth of 30 m and a distance of 100 m from the shore (Theodorou & Perissoratis, 1991). The sewage was flowing, without any treatment, directly to the sea through a diversion channel from the Keratsini outlet until 1994, when a biological treatment plant was installed. The effect of the sewage discharge was largely imprinted in the marine environment; it provoked a dramatic loss of clarity in the ambient water as well as a repulsive odor and the accumulation of organic-rich sediments on the seafloor (Theodorou & Perissoratis, 1991).

3 Materials and Methods

3.1 Fieldwork

The integrated marine geological survey of the Psyttalia–Keratsini Strait was organized in two phases. During the first phase, a marine geophysical survey was conducted using (i) a multibeam echosounder, (ii) two systems of subbottom profiling; a 3.5 kHz and a 600–2000 Hz Sparker system, and (iii) an EG&G 272TD dual-frequency (100/500 kHz) sidescan sonar. During the second phase, sediment cores were collected using a 3 m-long BENTHOS gravity corer. Trimble Differential GPS of RMS ± 1 accuracy was used for the survey.

The subbottom profiling systems were used to evaluate the thickness of the organic mud layer covering the natural sediments of the seabed. The high resolution 3.5-kHz profiler showed limited to no penetration into the seabed due to the high gas concentration in the surface organic mud layer. Low-frequency sparker profiler showed poor penetration allowing the rough estimation of the thickness of the organic mud. Six sediment cores, of about 90–130 cm long and 74 mm in diameter were collected. The sampling sites were chosen based on the results of the marine geophysical survey (Fig. 1).

3.2 Laboratory Techniques

3.2.1 Sedimentology

The retrieved sediment cores were stored vertically at 4 °C. Prior to analyses, they were gently cut longitudinally with Plexiglas sheet, measured, and photographed. The sedimentological investigation was based on macroscopic description and granulometry. The cores were visually described in terms of color and textural features. The visual core description was essential for determining the final number of samples for analyses in each core. Grain size analysis was carried out using the pipette-sieving method (Folk, 1974), while the statistical mean size (Mz) was calculated for each sample (totally 53 samples from all cores). Sediment classification was based on Folk (1974) nomenclature.

3.2.2 Chemical Treatment

Bulk geochemistry analyses and Organic Carbon (Corg) determination were applied in the studied sediments (Fig. S1 Supplementary material). The total number of analyzed samples for each technique was decided on the combination of macroscopic description, acoustic (geophysical) profile, and downcore sediment availability so that all the different lithological intervals could be efficiently represented for each core.

Elemental Analysis Two analytical techniques were employed to determine the elemental composition along the sediment cores. Inductively Coupled Plasma-Mass Spectrometry (ICP-MS) was applied on cores C1, C3, C4, and C6 (32 samples in total) for determining the following metals: Cu, Zn, Pb, Co, Mn, Ni, As, Ag, Cd, Cr, and Mo, while Atomic Absorption Spectrometry (AAS) was used in all 6 cores (50 samples in total) and defined the concentration of Cu, Zn, Pb, Co, Fe, Mn, Ni, Fe, and Ca.

Geochemical analysis was conducted by total digestion using HNO_3, $HClO_4$, HF, HCl 4 M, and HCl 0.3 M. Specifically, after removal of organic matter with H_2O_2 digestion, 0.1 g of each sediment sample was transferred into a Teflon tube and a mixture of concentrated HNO_3, $HClO_4$, and HF (2/1/5) was added and heated first in an open system for 3 h at 90 °C, then 3 h at 130 °C, 10 h at 190 °C, and finally 1 h at 90 °C. After cooling at room temperature, 2 mL of 4 M HCl was added and heated for 1:30 h at 70 °C. Again, after cooling at room temperature, 8 mL of 0.3 M HCl was added. Finally, the digests were filtered using millipore polycarbonate 0.45-μm filters and diluted up to 10 mL with ultrapure water and kept at 4 °C for subsequent elemental analysis.

Concerning AAS, elemental analysis in the solutions was utilized using a Perkin-Elmer 3100 atomic absorption spectrophotometer equipped with a deuterium/tungsten background corrector, corrosion-resistant nebulizer, and an N20 burner head. On the other hand, a Perkin-Elmer 6100 ICP-MS, equipped with a standard pneumatic nebulizer and an automatic sampler was used for ICP-MS measurements. Indium was used as the internal standard in order to correct potential instrument drift. Three reagent blank samples were run in the same way as the analyzing samples and the concentrations were determined using standard solutions. The detection limit range was 1–100 ppb for the AAS analysis and 0.001 ppt–1 ppb for the ICP-MS.

The two methods were compared using the exported concentrations of Cu, Pb, Ni, and Mn. The correlation diagrams showed good agreement for both methods (Fig. S2, Supplementary data). Nevertheless, it is obvious that concentrations of Pb determined using AAS are slightly higher than those determined by ICP-MS. Similar conclusions are deduced for Ni measurements (Fig. S2c, Supplementary data), but with a lower deviation between the two methods. On the contrary, comparing Mn concentrations, it seems that for low concentrations, AAS determines higher values than the ICP-MS and the opposite for high Mn concentrations (Fig. S2d, Supplementary data). Thus, the mean values of the elements were used as a normalization method.

Organic Carbon (Corg) Thirty five (35) samples were selected for the determination of the organic carbon content. Corg % was determined in the above samples using the Walkley–Black titration method, which is a classic method for the organic carbon analysis in sediments and soils (Walkley, 1947). The above method is based on the partial wet oxidation of the organic matter of the samples by a mixture of potassium dichromate with concentrated sulfuric acid followed by titration of the excessive dichromate by ferrous ammonium sulfate. Two standard samples were used for every 10 samples for organic carbon analysis as referred to Papaeyfthimiou et al. (2017).

3.3 Contamination assessment

3.3.1 Enrichment Factor

The degree of sediment contamination was assessed using the enrichment factor (EF) (Barbieri, 2016). The deeper sections of the cores collected closer to the island of Psyttalia correspond to the natural seabed. Therefore, the metal concentrations in the deepest sediments of these cores could be used as a reference to evaluate the metal pollution of the organic mud sediments (Barbieri, 2016). The enrichment factor (EF) was calculated in accordance with Hornberger et al. (1999) as follows $EF = C_i / C_{background}$, where C_i is the metal concentration in the sample, and $C_{background}$ is the total metal background value calculated in the

natural sediments from the bottom samples of the cores.

3.3.2 Geo-accumulation Index (I_{geo})

Geo-accumulation index is a valuable tool to quantify metal pollution and characterize its intensity in contaminated sediments. The I_{geo} values for the studied metals were calculated using the Muller (1979) formula: $I_{geo} = \log_2(C_n)/1.5*(B_n)$, where C_n is the measured content of element "n", and B_n is the background value of the "n" element.

3.3.3 Pollution Loading Index (PLI)

Pollution Loading Index (PLI) is defined as the nth root of the multiplications of the contamination factor of metals (CF). $PLI = (CF_1 \times CF_1 \times CF_1 \times \ldots \times CF_n)^{1/n}$, where CF_{metals} is the ratio between the content of each metal to the background values (background value from the natural sediments collected from the cores further from the sewage outfall) in sediment; $CF_{metals} = C_{metal}/C_{background}$. Therefore, PLI value of zero (0) indicates excellence; a value of one (1) indicates the presence of only baseline level of contamination while values higher than one (> 1) indicate progressive deterioration of the environmental conditions and increasing pollution (Tomilson et al., 1980). The PLI yielded an evaluation of the overall toxicity status of the sediments.

3.4 Statistical Treatment

Multivariate statistical analysis (Factor analysis) was performed in order to investigate the interrelationships between metals while also exploring their origin, geochemical behavior (Coxon et al., 2016; Li et al., 2020), and/or possible common sources. For this purpose, the statistical software program IBM SPSS v25 was used. The spatial (vertical) distributions of factor scores were plotted using the Ordinary Kriging (point Kriging) interpolation method in Surfer 11 software package (Golden Software Inc., USA). In this study, the multivariate method was applied to a dataset (14×32) consisting of Corg, Ca, and 12 heavy metals concentrations (As, Ag, Cd, Cr, Mo, Mn, Zn, Cu, Pb, Co, Ni, Fe) measured on 32 sediment samples from cores C1, C3, C4, and C6.

3.4.1 Factor Analysis

Factor analysis is a generic term that describes a number of mathematical methods designed to analyze interrelationships within a set of variables (R-mode) or objects (Q-mode) (Davis, 1986). The factors are constructed by a linear transformation of the original variables/objects in a way that reduces the overall complexity of the original data.

3.4.2 R-mode Factor Analysis

R-mode factor analysis aims to represent a large number of variables in the original data by a significantly smaller number of "factors", each of which is a linear function of the original variables. The R-mode dataset in this paper was constructed with columns containing Corg, Ca, and metal sediment composition and rows containing the samples number. For the selection of the "correct" number of factors, a combination of the common criteria was used (Davis, 1986). The Varimax procedure was used for the rotation of the retaining factors in order to achieve a "simple structure" which means producing as many loadings of near-zero and high. For purposes of interpretation of the Psyttalia–Keratsini strait dataset, "high" loadings were defined as those greater than 0.75, and "moderate" loadings were those between 0.40 and 0.75. Thus, variables that displayed rotated loadings greater than 0.40 were considered significantly loaded for a factor. Samples showing positive factor scores are mostly expressed by the positive loadings of the corresponding factor; similarly, samples with negative scores are expressed by the negative loadings, and samples with near-zero score values seem to not be affected by the corresponding factor. In the case of a bipolar factor, which contains extreme positive and negative loadings, high positive factor scores are related to the positive pole and high negative scores to the negative pole.

3.4.3 Q-mode Factor Analysis

Q-mode factor analysis is designed to portray interrelationships between objects (samples) on the basis of several properties (variables). The aim of Q-mode is (a) to determine the number of end members (factors) needed to account for the compositional variation observed; (b) to identify the end-member

samples, and (c) to calculate the proportion of each sample attributable to each member (factor loadings). For Q-mode factor analysis of Psyttalia-Keratsini strait sediments, a database was constructed so that columns contained the number of samples and rows contained Corg, Ca, and metal composition of the samples. A great number of similarity coefficients have been proposed but the most commonly used is the cosθ (Imdrie & Purdy, 1962). In order to fulfill the aims of the Q-mode factor analysis, as outlined above, a plot of factor loadings for the first two factors was used. The Varimax procedure was also used for the rotation of the retaining factors.

4 Results and Discussion

4.1 Geophysical

The bathymetric data showed that seafloor morphology is smooth, in the form of a broad valley with a maximum water depth of 40 m. The axis of the valley has a NE-SW orientation and the seafloor gently dips to the south. On the contrary, Psyttalia and Keratsini slopes display increased values (13% and 11% respectively). The examination of high resolution 3.5-kHz seismic profiles revealed the existence of a very prolonged surface echo of the seabed with no subsurface reflectors or very limited penetration underneath the seabed surface (Fig. 2a, b). The very prolonged surface reflection from the seabed covered by very soft mud suggests that the high reflectivity is not related to the granulometric properties of the seabed surface but, instead, to very poorly consolidated gassy sediments. The organic mud covering the seafloor is characterized by high percentages of Corg. The anaerobic degradation of organic matter produces gas (H_2S, CH_4) leading to acoustic masking in the 3.5-kHz subbottom profiling system (Papatheodorou et al., 1993). The low-frequency Sparker subbottom profiles exhibit higher penetration into the gas-charged organic mud (Fig. 2c, d). The combined interpretation of both seismic datasets allowed us to distinguish four areas, within the survey area, in terms of the thickness of

Fig. 2 Seismic profiles of the study area. The very prolonged surface echo of the seabed (**a**, **b**) is recorded using a 3.5-kHz subbottom profiling system, (**c**) and (**d**) correspond to low-frequency Sparker subbottom profiles
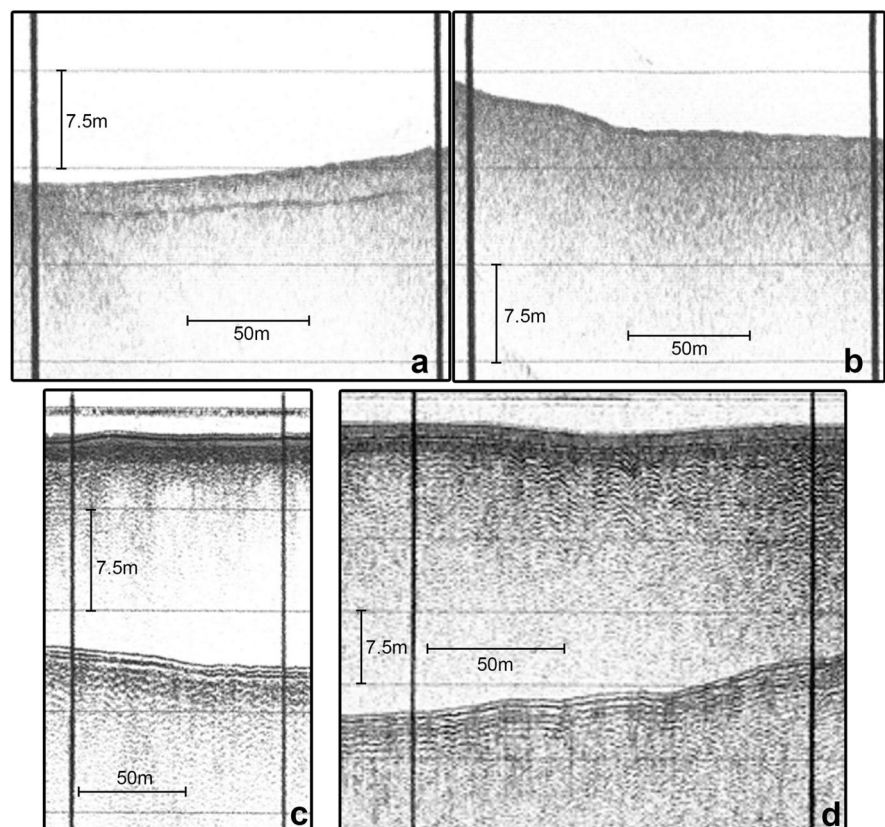
the organic mud layer (Fig. 1). Area A is characterized by a thickness of more than 1 m, with an estimated maximum thickness of about 2 m, Area B by thickness less than 1 m, Area C represents the geological background of the Psyttalia-Keratsini strait, while Area D stands for seabed more or less free of organic mud (Fig. 1).

4.2 Lithological Inspection

The macroscopic observations of the six collected cores (C1, C3, C4, C5, C6, and C8) discriminate the organic mud layer which overlies the natural sandy seafloor. The absence of natural sediments in the longest core C8 (130 cm) indicates that the organic mud layer is thicker than 130 cm. The natural sediments were collected in 3 cores C1, C3, C4 demonstrating a thinning of the organic mud layer with increasing distance from the sewage outfall. Sand intercalations were also observed within the organic mud layer (cores C1 and C3). The thickness of the

organic mud layer observed in the core sediments is in accordance with the thickness that has been estimated by the marine geophysical survey (Fig. 3).

The organic mud layer's color varies from gray to black. Additionally, small pieces of litter were spotted within this layer. The underlying natural sediments include biogenic material consisting mostly of gastropod fragments.

4.2.1 Grain Size Spatial Distribution

Grain size analysis indicates the differentiation between the organic mud samples and those of the natural sediments. Silt fraction dominates in organic mud (56.37%), on the contrary, in the underlying natural seafloor, sand is the dominant fraction (54.44%), but silt displays a large percentage as well (Table S1, Supplementary data). Moreover, sand fraction values are significant in cores C1 (44.27%) and C3 (27.87%) that were collected further from the outfall. The silt fraction dominates in almost every core with
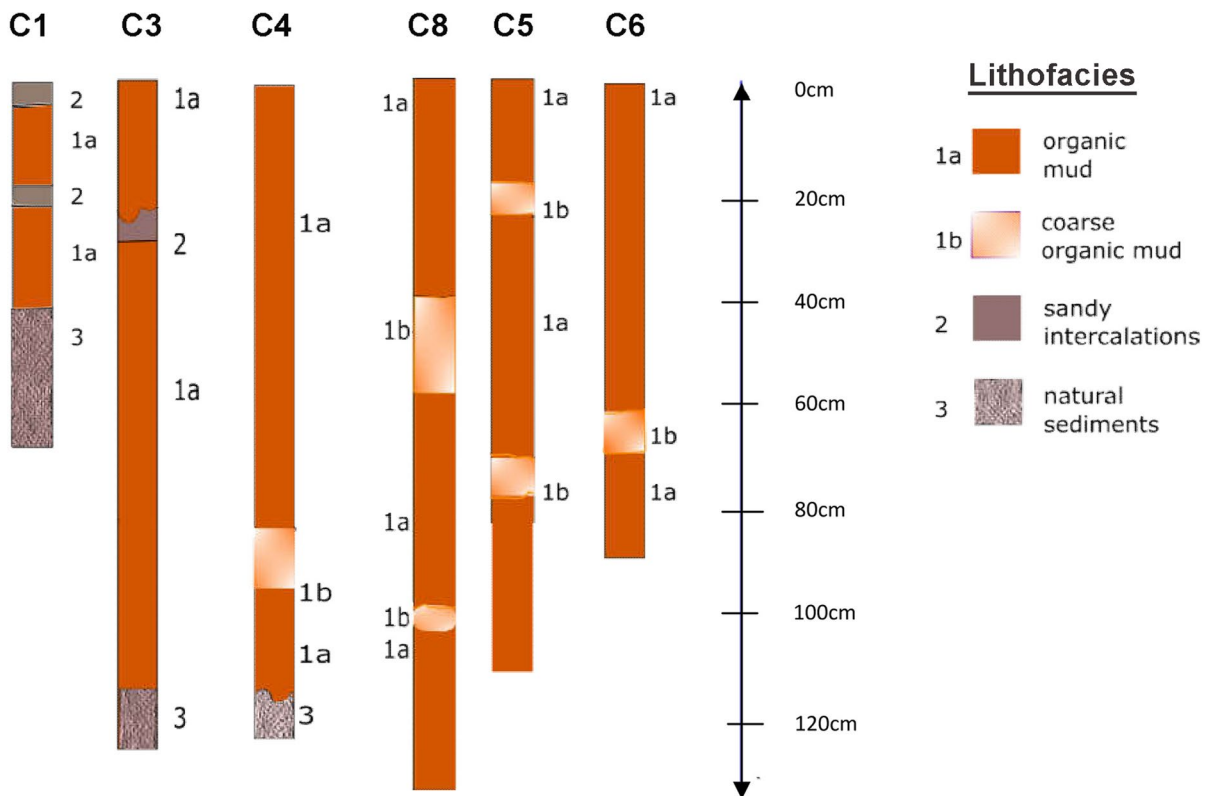

Fig. 3 Distribution of identified lithofacies along the studied cores

its higher participation in the sediments collected in cores C4 (71.40%) and C6 (57.77%) (Table S1, Supplementary data). Figure 4a, b, c and d represents the spatial distribution (cross-sections) of sand, silt, clay percentage fractions and Mean size (Mz) in the overall sedimentary succession of the strait. The gravel fraction due to its very small participation in the sediments is not represented here. The highest concentrations of sand (> 30%) can be observed at a distance of 550 m from the outfall, closer to Psyttalia (core C1). These percentages can be noted in three layers; one surficial, one in a depth of 30 cm, and another in the deepest sediments of the core. It can be concluded that they represent natural sediment layers.
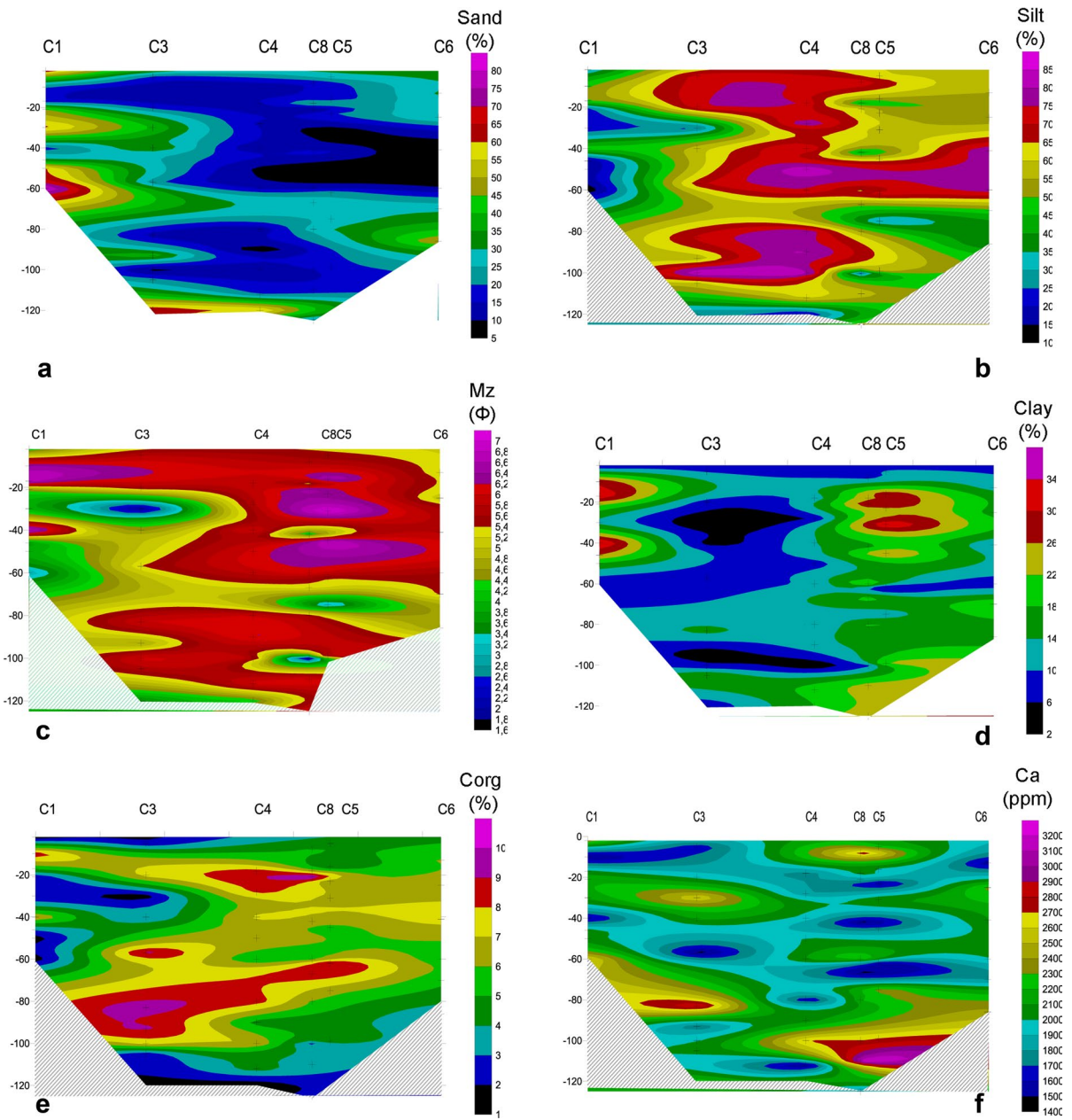
Fig. 4 Cross sections of **a** sand, **b** silt, **c** Mz, **d** clay, **e** Corg, and **f** Ca distributions in the sediments of Psyttalia-Keratsini strait

On the contrary, closer to the outfall (cores C4, C5) high sand fraction percentages are noted deeper than 1 m delimiting the above organic mud layer from the natural sediments. In general, the sand fraction is higher with increasing distance of the sewer while it displays its lowest percentages in the middle of the Keratsini-Psyttalia distance. The exact opposite trend is observed in Fig. 4b, where the vertical distribution of silt fraction is represented, underlining the negative correlation of the two fractions.

Clay fraction displays its higher percentages in cores C8, C5, and C6. Two clay intercalations can also be noted in core C1 which is the most distant core from the outfall (Fig. 4d). It should be also noted that sand intercalations appear in cores C1 and C3. All the above indicate that possible mixture processes take place between natural sediments and the organic mud with increasing distance from the outfall. The cores C1 and C3 were collected downslope of the slope of Psyttalia so the sand intercalations may be interpreted as storm deposits. Finally, the spatial distribution of Mz exhibits significant fluctuation (1.7–7.08 Ø) suggesting an intense hydrodynamic variability along the Keratsini-Psyttalia strait. Notably, the Mz distribution coincides with that of silt which is the dominant size fraction (Fig. 4b and c).

4.2.2 Lithofacies

The macroscopic observations along with grain size analysis allowed the identification of four (4) different lithofacies along the retrieved cores as shown in Fig. 3.

Lithofacies 1 a: it consists mostly of slightly gravely mud of light to dark brown or black color that suggests a high content of organic matter. Litter, threads, and plant residues were spotted. The mean percentages of gravel, sand, silt, and clay are 1.96%, 22.20%, 59.47%, and 16.37%. The thickness of lithofacies 1 a, varies from 133 cm (closer to Keratsini slope) to 42.5 cm (near Psyttalia slope). Therefore, lithofacies 1 a, corresponds to the organic mud layer.

Lithofacies 1 b: intervals of coarser sediment deposits of relatively similar characteristics with the previous lithofacies were discriminated and classified as lithofacies 1 b intervals. It mostly comprises gravelly to sandy mud of light brown color and plenty of filaments and litter. Its mean thickness is estimated to be 10 cm and the mean percentages of gravel,

sand, silt, and clay are: 12.2%, 20.62%, 49.84%, and 16.61%. This layer is collected in cores C8, C5, and C6 which were collected closer to Keratsini and the sewage outfall. This lithofacies can be considered as a coarse organic mud layer.

Lithofacies 2: relates to sandy mud layers of gray color. It is identified in cores retrieved closer to Psyttalia and mean percentages of gravel, sand, silt, and clay are 12.50%, 52.88%, 23.78%, and 10.84%, respectively. Thus, a mean thickness of about 20 cm represents sandy intercalations within the organic mud layer attributed possibly to storm events or events triggered by anthropogenic activities.

Lithofacies 3: corresponds to slightly gravely sand of gray color and appears in the base of cores C1, C3, and C4. This layer was present only close to the island of Psyttalia and is also characterized by the presence of gastropods. The mean percentages of gravel, sand, silt, and clay fractions are 7.73%, 54.44%, 25.84%, and 11.99%, respectively. These lithofacies represent the natural sediments of the survey area.

4.3 Geochemistry

4.3.1 Metal Concentrations in Psyttalia-Keratsini Sediments

Heavy metals, Ca, and Corg concentrations in the sediment cores C1, C3, C4, C5, C8, and C6 are presented in Table S2 (Supplementary data) along with their minimum, maximum, and mean values. Elements that were determined using both AAS and ICP-MS (Cu, Zn, Pb, Co, Mn and Ni) are referred to as mean and presented by the average values. Mean metal concentrations and Corg in the organic mud layer and natural sediments (associated with the lithofacies identification) are shown in Table 1. Organic mud deposits are characterized by higher concentration values for all metals and Corg compared to those of the natural sediments (Table 1). The lithofacies 1 a (associated with organic mud) shows higher concentrations of Cu, Zn, Pb, Ag, Cd, Cr, Mo, Fe, comparable concentrations for Corg, Ca, Co, Mn, Ni, and lower concentrations of As compared to those of lithofacies 1 b (coarse organic mud) (Table 1).

Subsurface sediments collected at the base of the cores C1 (C1/9) and C3 (C3/10) are non-polluted sediments and their concentrations were considered, consequently, as background concentrations for the

Table 1 Organic Carbon (Corg) and metal average values in the four lithofacies as well as in total, organic mud and natural sediments of the Psyttalia-Keratsini strait

	Lithofacies 1a	Lithofacies 1b	Lithofacies 2	Lithofacies 3	Total	Organic mud	Natural sediments
Corg (%)	5.80	5.38	1.78	1.37	5.47	5.70	1.05
Ca (ppm)	1988.03	1973.50	2319.00	2350.33	2046.32	2025.04	2447.00
Cu (ppm) mean	214.19	168.58	80.38	16.40	196.40	187.89	5.60
Zn (ppm) mean	1627.58	1278.92	1000.75	111.17	1441.61	1281.73	66.00
Pb (ppm) mean	326.19	260.50	155.88	72.22	296.80	298.31	42.08
Co (ppm) mean	18.90	19.91	13.61	13.89	19.04	20.72	13.14
Mn (ppm) mean	181.54	186.17	145.00	134.50	175.84	176.47	114.25
Ni (ppm) mean	86.69	84.33	55.13	32.67	81.66	81.35	21.75
As (ppm)	61.49	100.00	48.55	47.00	61.21	63.59	26.25
Ag (ppm)	12.59	8.89	4.08	0.91	10.86	11.70	32.50
Cd (ppm)	3.93	3.23	1.76	0.46	3.50	3.76	0.29
Cr (ppm)	704.22	524.50	298.50	88.23	620.52	663.99	77.00
Mo (ppm)	6.30	2.69	4.33	0.80	5.59	5.94	0.33
Fe (ppm)	13,210	12,250	11,630	8530	12,230	12,550	5950

evaluation of the metal pollution in terms of enrichment factor (EF), geo-accumulation Index (I_{geo}), and Pollution Loading Index (PLI). The mean and maximum heavy metal concentrations in the organic mud layer (Lithofacies 1 a and 1 b) are among the higher measured in Greece and comparable or lower to those in other polluted gulfs and ports, worldwide (Table 2). Compared to average shale values, concentrations of As, Cd, Cr, Cu, Ni, Pb, and Zn are substantially higher. Additionally, minimum concentrations of the above elements are lower than the global standards indicating that some samples are not/or less impacted (Table 2). Finally, metal concentrations of the present study are comparable to those determined in North Saronikos Gulf by previous studies (Table 3).

4.3.2 Organic Carbon (Corg) and Calcium (Ca) Spatial Distribution

Vertical distribution (cross-section) of organic carbon (Fig. 4e) in all sediment cores can provide useful information on the pollution history of the area between Psyttalia and Keratsini. The organic carbon distribution defines the organic mud layer that has been deposited due to the operation of the sewage outfall. Corg concentrations are low (2–3%) in the deeper sediments of cores C4, C3, and C1, where, natural sediments were dominant. Similar low Corg percentages have been noted in the surface and between 20–30 cm below the seafloor close to Psyttalia side. The latter coincides well with the prevalence of sand intercalations that have been found in those depths (Figs. 3, 4a).

With the exception of the above-mentioned layers, all the organic mud deposits are characterized by high Corg concentrations (3–10%) with a slightly decreasing trend toward the Psyttalia coast and away from the outfall (Fig. 4e). The highest Corg concentrations (> 6%) are observed in two layers; (i) a deep layer at 70–90 cm depth, and (ii) a shallow layer at 10–30 cm below the seabed. The cross-section of Corg exhibits high similarity with that of silt fraction (Fig. 4b) and to a lesser extent to that of clay (Fig. 4d). On the contrary, Corg cross-section shows an inverse pattern with that of sand, suggesting a negative correlation between Corg and sand (Fig. 4a).

The calcium cross-section in the sediment of the strait shows a different pattern compared to that of Corg (Fig. 4f). Given also the lithological inspection of the cores (Fig. 3), elevated Ca percentage values are observed in layers of organic mud (Lithofacies 1 a) but also in coarse organic mud (Lithofacies 1 b) and sand intercalations (Lithofacies 2) suggesting different sources of calcium in the organic mud deposits and the natural sediments of the survey area.

Table 2 Ranges and mean values (min–max/(mean)) of element concentration (mg kg^{-1}) in sediment of Psyttalia-Keratsini strait compared with different Greek, Mediterranean, European and worldwide harbors reported in the literature (values in mg/kg^{-1}). The average shale concentrations and the sediment quality guidelines are also given

Location	Method	As	Cd	Cr	Cu	Ni	Pb	Zn	Ref
Psyttalia_Keratsini	Total extraction, HClO$_4$, HNO$_3$ and HF	30.2–194.00 (61.21)	0.20–7.23 (3.50)	76–1089.0 (620.52)	4.45–404 (196.40)	8.50–129.00 (81.66)	40.0–645.50 (296.80)	57.0–4742.0 (1441.61)	This study
Patras Harbor	Total extraction, HClO$_4$, HNO$_3$ and HF	4.16–13.20 (8.15)	0.22–0.73 (0.33)	180–230 (199.6)	30–128 (59)	56—140 (101)	19–128 (37)	55.2–343.0 (106)	Papaefthymiou et al., 2010
Gulf of Patras (outside the harbor)	Total extraction, HClO$_4$, HNO$_3$ and HF	-	(0.44)	(145.0)	(37.0)	(18.0)	(29.0)	(261.0)	Leotsinidis & Sazakli, 2008
Thermaikos Gulf, Greece	HNO$_3$ and HCl (except for the silicate fraction)	-	-	7–172 (47)	19–165 (80)	-	10–218 (77)	74–358 (184)	Christophoridis et al., 2009
Rhodes harbor, Greece	0.5 N HCl (extractable fraction)	-	0.003—0.08 (0.05)	32–77 (59)	38.3–101.0 (65)	-	78–152 (135)	59–168 (145)	Angelidis & Aloupi, 1995
Naples harbor, Italy	Total extraction, HClO$_4$, HNO$_3$ and HF	1–1121	0.01–3	7–1798	12–5743	4–362	19–3083	17–7234	Sprovieri et al., 2007
Port of Bagnoli, Italy	Total extraction, HClO$_4$, HNO$_3$ and HF	0.5–4.0 (2.0)	0.01–3.24 (0.57)	4–54 (28)	0.5–126.1 (27.2)	0.01–52.5 (6.93)	52–896 (221)	91–2313 (602)	Romano et al., 2004
Cádiz Harbor, Spain	HNO$_3$ and aqua regia	3.4–30.7 (14.7)	0.92–1.3 (1.2)	0.1–14.9 (9.4)	7.0–202.8 (72.2)	0.06–21.3 (14.6)	2.3–86.9 (28.0)	21.27–378.3 (150.2)	Casado-Martnnez et al., 2009
Barcelona Harbor, Spain	HNO$_3$ and aqua regia	17.4–29.0 (21.5)	0.62–2.9 (1.5)	59.5–105.2 (90.6)	74.9–601.1 (234.5)	18.9–32.3 (25.63)	86.7–455.3 (184.3)	219.7–1165 (515.6)	«
Cartagena Harbor, Spain	HNO$_3$ and aqua regia	62.6–101.5 (79.2)	6.8–98.5 (38.7)	29.5–66.64 (49.8)	171.1–665.9 (400.9)	15.3–29.0 (20.8)	486.7–1397 (1007)	900.8–8661 (3689)	«

Table 2 (continued)

Location	Method	As	Cd	Cr	Cu	Ni	Pb	Zn	Ref
31 Dutch harbors (The Netherlands)	Extraction with HNO$_3$ and HCl	<4–69	<0.3–8.4	<15–200	<5–180	<3–80	<5–250	<10–1000	Stronkhorst & Hattum, 2003
Rotterdam harbor (The Netherlands)	Dutch standards NEN 5770	-	0.6–1.8		20–40	9–20	40–60	120–190	Van den Hurk et al., 1997
East London and Elizabeth Harbor, South Africa	Total extraction, HClO$_4$, HNO$_3$ and HF	-	100–1630		8600–183,000	-	9–84,200	18,800–332,000	Fatoki & Mathabatha, 2001
Montevideo harbor, Uruguay	HNO$_3$	-	1.0–1.6	79–253	58–135	-	44–128	174–491	Muniz et al., 2004
Boston harbor, USA	Cold HCl and hot HNO$_3$/HCl	-	-	-	7–142	-	18–263	39–414	Zago et al., 2001
Tolo Harbor, Hong Kong	Extraction with HNO$_3$ and HCl	-	-	14–30	21–84	-	48–144	100–270	Owen & Sandhu, 2000
Victoria Harbor, Hong Kong	Digestion with HNO$_3$ and HClO$_4$	-	-	-	16–280	-	21–85	52–221	Tang et al., 2008
Sydney harbor, Australia	2:1 HClO$_4$/HNO$_3$	-	-	-	9.3–1053	-	38–3604	108–7622	Birch & Taylor, 1999
Average shale		13	0.3	90	45	68	20	95	Wedepohl, 1969
Sedimet Quality Guideline (ERL–ERM)		8.2–70	1.2–9.6	81–370	34–270	20.9–51.6	46.7–218	150–410	Long et al., 1995

4.4 Source Identification

The results of the R-mode factor analysis led to the discrimination of geochemical processes along the sedimentary successions and allowed the identification of possible sources from which the metals derived into the Psyttalia-Keratsini strait. Four (4) factors were utilized to describe the interrelations among the variables. The definitive factor model explains the largest part of the total variance of the original dataset (86%) and can be considered statistically significant (Table 4). Moreover, the high communalities (>0.70) for all variables suggest that the factor model expresses well the analyzed variables. The above mentioned suggest that the four-factor model efficiently explains the downcore geochemical variations of all original variables and can be used to define the interrelations of the

Table 3 Ranges and mean values (min–max/(mean)) of element concentration in the sediment of North Saronikos Gulf reported in the literature (values in mg/kg)

Method	As	Cd	Cr	Fe	Pb	Zn	Cu	Co	Ref
Total extraction, HClO$_4$, HNO3 and HF	30.2–194.00 (61.21)	0.20–7.23 (3.50)	76–1089.0 (620.52)	4200–29,000 (12,230)	40.0–645.50 (296.80)	57.0–4742.0 (1441.61)	4.45–404 (196.40)	10.4–38 (19.04)	This study
INAA	0.7–70		35–1000			45–1800			Papakostidis et al., 1975
INAA	100		1100	40		1800		18	Grimanis et al., 1977
0.05N HCl 0.025 N H$_2$SO$_4$ (A.A.S)				0,71		630	58		Voutsinou-Taliadouri, 1981
Nearly total extraction, KNaCO$_3$ and HCl	66–1813 (471)	190–1763 (998)	264–860 (463)		521–1263 (648)	409–6725 (1435)	195–518 (288)		Galanopoulou et al., 2009

geochemical phases, without losing any important information.

Factor 1 explains the largest proportion of the total variance (57.73%) of the original variables and exhibits high positive loadings for Ag, Cd, Cr, Cu, Zn, Pb, Mn, and Corg (Table 4). Factor 1 is considered to be an organic-metal pollutant factor that reflects the complexation processes between the majority of heavy metals and organic matter (Saxby, 1973; Zhang et al., 2014) while also provides information about the contamination caused by the untreated sewage discharged in the area for over 40 years. Anthropogenic sources of metals and Corg include municipal-domestic sewage and industrial wastewaters (Mara, 2003). Domestic sewage is a mixture of waste waters and certain amount of organic and inorganic contaminants in dissolved, suspended, and colloidal states, including various heavy metals (Mara, 2003). Industrial wastewaters contain high amount of heavy metals (Azimi et al., 2017), while in many cases of large cities, these wastewaters get mixed in the local sewage system (Bincy et al., 2015). In the case of Psyttalia–Keratsini strait, potential metal sources related to industrial activities comprise tanning, dyeing, paper cement, insecticides, fertilizers, plastics, chemicals, and food processing plants. Another potential source for lead (Pb) is also gasoline since road washout discharged together with domestic sewage (Kersten et al., 1997). Silver (Ag) concentrations can be

attributed to the fact that Ag was broadly used in photographic films, silverware, jewelry, coins, and, in most recent years, of the outfall operation in electrical and electronics (Dixit et al., 2015). Another metal of many uses is Copper (Cu), but the main source of municipal waste in the area seems to be the water supply system of the city of Athens due to copper water pipes (Boller & Steiner, 2002). Moreover, Cadmium (Cd) could participate in municipal waste due to packaging usage, ceramics dyeing, and in most recent years, in detergents and batteries (Dasenakis et al., 2015; Dixit et al., 2015). It should be noted that among the metals correlated with Factor 1, the metals Ag, Cr, Cu, and Zn exhibit high positive loadings solely in this factor (Table 4). On the contrary, Cd, Pb, and Mn show significant positive loadings at more than one factor suggesting the multisource origin of these metals (Table 4).

The positive scores of this organic-metal pollutant factor dominate the major part of the cross-section; especially the part which is closer to the outfall at Keratsini (Fig. 5a). The surface organic mud layer close to the outfall is also characterized by positive factor scores while the surface layer at the Psyttalia side shows negative factor scores suggesting that the organic-metal pollutant factor has a weak effect on the Psyttalia shelf (Fig. 5a). The most striking finding is that the maximum factor scores — which are located between 20 and 50 cm in C4 and between 50

Table 4 Varimax rotated factor loadings (R-mode) for raw datasets and eigenvalues, percentage and cumulative percentage explained by each factor

| | Rotated component matrix | | | |
| | Component | | | |
	1	2	3	4
Corg (%)	0.919	− 0.067	0.081	− 0.141
Ca (ppm)	− 0.361	− 0.404	− 0.301	0.625
Cu (ppm) mean	0.772	0.302	0.491	0.178
Zn (ppm) mean	0.840	0.059	− 0.162	− 0.070
Pb (ppm) mean	0.701	0.595	0.294	− 0.064
Co (ppm) mean	0.039	0.147	0.916	− 0.034
Mn (ppm) mean	0.532	0.450	0.469	− 0.231
Ni (ppm) mean	0.452	0.272	0.710	− 0.249
As (ppm)	− 0.075	0.941	− 0.001	− 0.111
Ag (ppm)	0.862	0.010	0.369	− 0.089
Cd (ppm)	0.686	0.504	0.389	0.073
Cr (ppm)	0.874	0.098	0.400	− 0.023
Mo (ppm)	0.440	0.327	0.493	0.445
Fe (ppm)	0.099	0.857	0.426	0.002
	Total variance explained			
	Component			
	1	2	3	4
Initial Eigenvalues	Total	8.082	2.157	1.062	0.723
	% of Variance	57.727	15.410	7.585	5.161
	Cumulative %	57.727	73.137	80.722	85.884

and 100 cm in C3 — form a certain layer at the middle part of the survey area (Fig. 5a). This layer represents an extended deposit that has been deposited under the high influence of this organic-metal pollutant factor.

Factor 2 explains a proportion of 15.41% of the total variance. This second factor displays high positive loadings for Fe and As and moderate positive loadings for Pb, Cd, and Mn (Table 4). This is also a metal pollution factor which, however, does not correlate with Corg indicating probably a second pollution source in the area such as fertilizer and sulfuric acid plant with As-rich solid wastes (Angelidis & Grimanis, 1987). The high loadings of As (0.941) and Fe (0.857) in this factor, indicate the high correlation between As and Fe, a strong association that is well known and well-studied in marine sediments (Bataillard et al., 2014). Fe/Mn hydrous oxides appear to be the most important scavengers of As in polluted sediments (Angelidis & Grimanis, 1987; Crecelius, 1975). Arsenic is mainly associated with Fe, Mn, and Al-oxides in

oxic conditions. After burial, As is reduced to As (III) and simultaneously released into the porewater when Fe (III)-oxides are reduced in the sediments (Chaillou et al., 2003). Dissolved As can then diffuse upwards in the oxic zone of the surface sediments and get fixed onto particles by adsorption or co-precipitation. Alternatively, it can diffuse downwards to the zone of sulfate reduction and interact with dissolved or particulate sulphides (Mucci et al., 2000). The moderate loading of Pb in this factor probably indicates the pollution of the survey area by an iron and steel plant which was discharging particulate waste into a settling lagoon at the Northwestern part of Elefsis Bay until 1981 (Kersten et al., 1997).

The vertical distribution of the second factor's scores shows high and elevated values at the eastern part of the cross-section (cores C4 and C6) and at the deeper part of the organic mud deposits suggesting that a pollution source from the Keratsini and surrounding areas has influenced the deposits during the earliest stages of the function of the outfall (Fig. 5b).
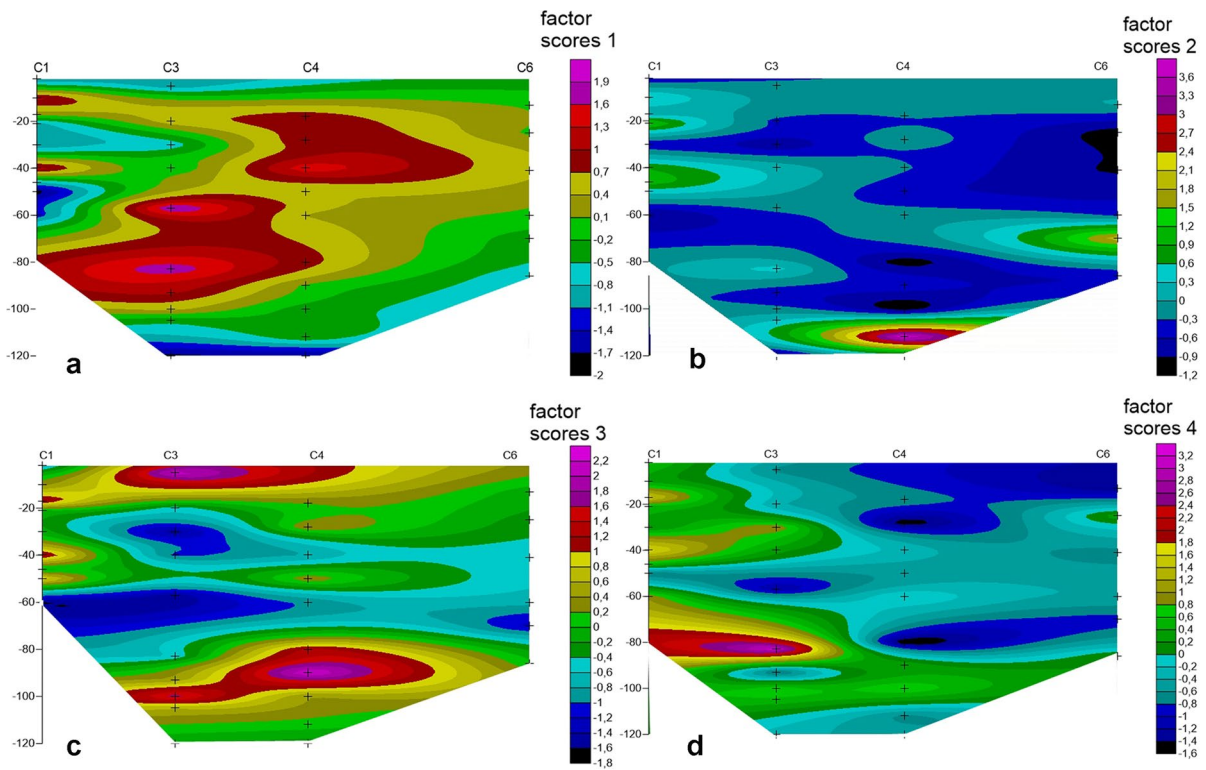
Fig. 5 Cross-sections of the four R-mode factor scores between Psyttalia and Keratsini

Factor 3 explains a significant proportion of the total variance (7.59%) and displays high positive loadings for Co and Ni (0.71–0.92) and moderate positive loadings for Mo, Mn, and Cu. Factor 3 can be considered as another metal pollution factor, but these metals are not associated with organic carbon, suggesting a different pollution source than domestic sewage, such as industrial inputs and factory waste or perhaps other nearby point sources i.e. fertilizer factory (Voutsinou et al., 1981), oil refineries and shipyards (Moore & Ramamoorthy, 1984).

The high values of factor 3 scores are observed in two layers; (i) a surface layer (0–50 cm) with the highest values at the upper 20 cm and (ii) a deep layer (80–120 cm) above the natural sediments (Fig. 5c) that coincide with Lithofacies 1 (a and b) intervals (Fig. 3). Thus, two periods of increased effect of factor 3 are implied; one at the beginning of the outfall function and another during recent years. Moreover, these two layers are located just above and underneath an interval of high factor 1 scores suggesting a

temporal variation of two factors, which both explain 65.32% of the total variance of the original dataset.

Factor 4 explains a small portion of the total variance (5.16%) and exhibits high positive loadings only for Ca; hence, it can be considered as a calcium carbonate factor. High and elevated factor scores are observed at the Psyttalia side of the cross-section in the unpolluted sediments underlying the organic mud layer and the sandy intercalations but also in the organic mud layer suggesting a multi-source input of calcium carbonate (Fig. 5d). Ca reflects the biogenic components of the studied sediments (bivalve shells, gastropods) as well as important detrital input, given the geological background of the area (Theodorou & Perissoratis, 1991). However, the moderate positive loading of Mo in this factor might relate with construction facilities in the cities of Athens and Piraeus; limestone quarries of Attica are located on massive carbonate platforms which accommodate molybdenite ores (Voudouris et al., 2010). Therefore, factor 4 could relate either to the deposition of natural (detrital and/or biogenic) sediments or to rinsing and

input of lime components in the Psyttalia-Keratsini area from the construction industries. It is most likely that the matching of high scores of factors 1 and 4 between 60 and 90 cm in core C3 (Fig. 5a, d), associated with the prevalence of Lithofacies 1 a (organic mud), reflects a rather anthropogenic source of calcium carbonate.

Figure 6a presents the specific layers in which the three most important factors (80.7% of total variance) express their major influence. This diagram can be interpreted in terms of the temporal variation of the prevailing pollution processes during the deposition of organic mud. At the early stage of the function of the outfall, the lower layer of organic mud has been mainly influenced by a Fe-As-Pb–Cd-Mn pollution process (Factor 2). Just above the early stage layer, the deposition of organic mud layer was influenced by the Co–Ni-Mo-Mn-Cu pollution process (Factor 3). After the two deposits of the early stages, the organic mud has been deposited under the influence of organic-metal pollutants factor (Ag-Cd-Cr-Cu–Zn-Pb-Mn-Corg, Factor 1), for a long period. Finally, Co–Ni-Mo-Mn-Cu pollution process (Factor 3) seems to be the main pollution mechanism of the recent stages of the deposition of organic mud and particularly the western part (Psyttalia) of the surface layer.

4.5 Contamination Assessment (Environmental Indices)

4.5.1 Enrichment Factor (EF)

Metal Enrichment Factor (EF) is used as an index to evaluate the anthropogenic influence of heavy metals in sediments. According to EF, the metals in the Psyttalia-Keratsini strait were found to be in the following order: Cu > Zn > Mo > Ag > Cd > Cr > Pb > Ni > Fe > As > Mn > Co (Table S3 Supplementary data). The minimum, maximum and mean enrichment factor values calculated for all the analyzed metals are given in Table S3 (Supplementary data) as well. Elements can be distinguished into three major groups with respect to their corresponding mean enrichment factors: Elements with enrichment which is not considered significant (EF < 5) such as Mn, Co, Fe, and As, elements with medium-level enrichment (5 < EF < 20) such as Ni, Cr, Pb, Cd, and Zn, highly enriched elements (20 < EF < 40) as Ag, Mo and finally, very
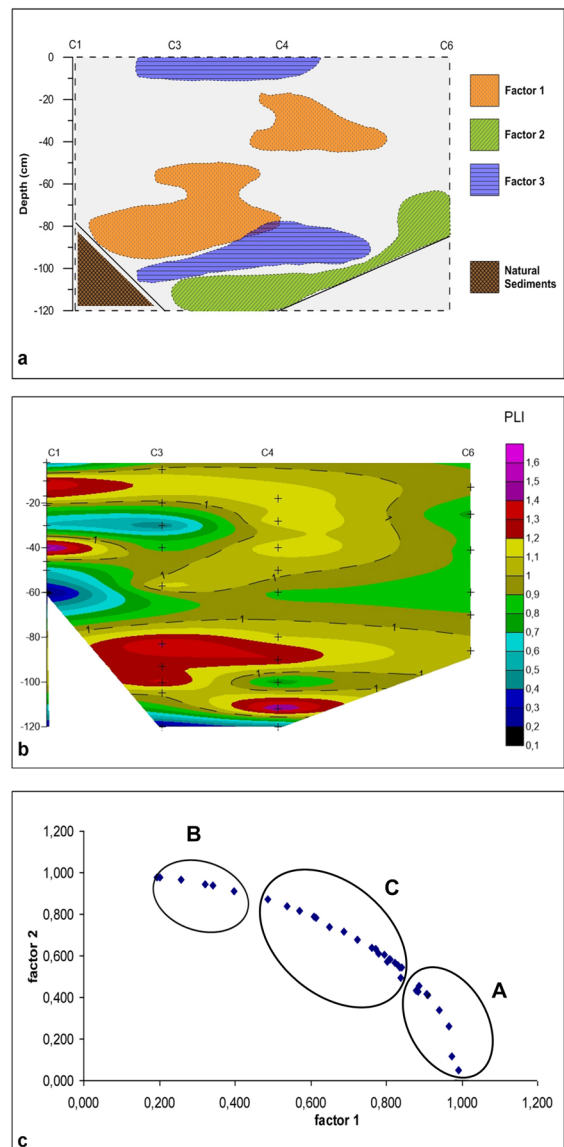
Fig. 6 a Distribution of maximum levels of the three (R-mode) factor scores (pollution factors) along the studied successions, **b** Cross-section of PLI, **c** Two factors plot obtained from Q-mode factor analysis indicating three different sample clusters A, B and C.

highly enriched elements as Cu (EF > 40) (Barbieri, 2016) (Table S4 Supplementary data). Metals with high and medium enrichment are clustered in the Factor 1 while metals with no significant enrichment in Factors 2 and 3.

4.5.2 Geo-accumulation Index (I_{geo})

Another criterion to evaluate heavy metal pollution is the Geo-accumulation index introduced by Muller (1979). There are seven classes describing the pollution rate for each metal (Table S4 Supplementary data). The results of I_{geo} values are presented in Table S5 (Supplementary data). According to the I_{geo} classes, the sediments of the organic mud layer between Psyttalia and Keratsini range from strongly polluted to extremely polluted in Cu. Moreover, sediments are strongly polluted in Ag, Mo, and Zn. Additionally, the area can be considered moderately to strongly polluted in Cd, Cr, and Pb. Sediments are also moderately polluted in Ni, unpolluted to moderately polluted in As, Fe, Mn, and, finally, unpolluted in Co (Table S5 Supplementary data). Thus, according to I_{geo} index, the metals can be ranked as Cu > Ag, Mo, Zn > Cd, Cr, Pb > Ni > As, Fe, Mn > Co.

4.5.3 Pollution Loading Index (PLI)

Pollution Loading Index (PLI) is a useful tool for assessing the overall degree of contamination in the organic mud layer. PLI values range from 0.13 to 1.6 with most of the samples exhibiting values greater than 1 (Fig. 6b). Although no clear PLI classes have been proposed for the assessment of the sediment contamination, many researchers suggest that PLI < 1 indicates unpolluted sediments while PLI > 1 indicates progressive contamination. The cross-section of the PLI values highlights two layers of PLI values greater than 1: (i) a surface layer (0–50 cm) with more contaminated deposits toward the western part (Psyttalia) of the area and (ii) a deep layer (80–110 cm) with more intense and widespread contamination (Fig. 6b). This PLI pattern suggests that the organic mud was more contaminated with metals during the early stage of the function of the sewage outfall.

4.5.4 Q-mode Factor Analysis

Q-mode factor analysis was performed on the transposed geochemical dataset that was analyzed also for R-mode. A total of 98.92% of the total variance of the original data set is explained by the first two Q-mode factors; 88.78% is explained by the first factor and 10.15% by the second factor (Table S6,

Supplementary data). The amount of variance explained by the first two Q-mode factors is slightly greater than that resulted from R-mode factor analysis. The normalized rotated factor loadings for the two Q-mode factors are shown in Table S7 (Supplementary data). The Q-mode factor loadings describe the relative proportion of the metal concentrations in the sediment samples.

The Q-mode factor loadings have been plotted in the two factors plot and a narrow band has been well developed, covering all the space between the two factors (Fig. 6c). Consequently, three groups of samples (A, B and C) were defined (Fig. 6c).

Examination of the end–member characteristics of groups A and B and samples proximal to them (group C), showed that group A contains highly polluted sediment samples, group B samples with minimum pollution load and group C is characterized by the intermediate degree of contamination. More specifically, group A shows much higher concentrations of Corg, Ag, Cd, Mo, Cu, Zn, Pb, Ni, and Fe compared to those of group B and higher than those of group C (Table S8, Supplementary data). On the contrary, group B contains sediment samples with the lowest metal concentrations, with the exception of the high Ca proportion, suggesting a correspondence to the natural sediments and/or slightly polluted sediments of the area (Table S8, Supplementary data).

Arsenic (As) and cobalt (Co) present a different behavior and show the highest concentrations in the intermediate group C. Notably, these two elements display their highest concentration values within the lithofacies 1 b intervals (Table 1). This observation underlines the differentiation of lithofacies 1 b which seem to represent less contaminated conditions compared to lithofacies 1 a. Indeed, group A sediment samples which are indicators of the highest pollution degree, correspond exclusively to lithofacies 1 a intervals and are located at the top 40 cm and between 80 and 100 cm below the seabed, matching perfectly with the aforementioned layers of the much-increased PLI values (Fig. 6b). Furthermore, these layers coincide with the maximum scores of factors 1 and 3 (Fig. 6a) reflecting the dominant contribution of copper (Cu) — which exhibits significant loadings for both factors — in the contamination degree of the studied sediments.

Sediment samples of group B are observed at the surface of the western part (Psyttalia) and at the base

of the cores (C1, C3, and C4) where natural sediments prevail.

5 Summary and Conclusions

Six (6) sediment cores were collected from Psyttalia-Keratsini strait, where, the central sewer of the Athens metropolitan area had been discharging untreated sewage from 1950 until 1995. The sediments were analyzed in terms of lithology, elemental, and Corg concentrations. Combined marine geophysical data and lithological inspection revealed the presence of an organic mud layer which gets thinner with increasing distance from the sewage outfall. The organic mud deposits display a high degree of enrichment in Cu, Ag, Zn, and Mo. The PLI values for the majority of the sediment samples are higher than 1, suggesting progressive contamination of the organic mud deposits by heavy metals.

The results of the geochemical analyses together with the Geo-accumulation Index (I_{geo}) and the Pollution Loading Index (PLI) calculations, and the application of multivariate statistical analysis, managed to predict the contamination history of the studied area. At the early stage of the outfall function, the lower layer of organic mud seems to be influenced by fertilizer and sulfuric acid plant activities. At the following stage, the organic mud deposition is related principally to industrial inputs and factory waste. A long period related to urban waste discharges lies above them and constitutes the more recent contamination in the studied area except the western part, where a Co–Ni–Mo–Mn–Cu pollution was observed at the surface deposits.

The findings of this work contribute to the baseline information regarding sediment contamination in a gulf influenced by several sources of pollution (municipal and industrial). In such areas, the monitoring of the sedimentary deposits, with the combined application of laboratory analytical and marine remote sensing techniques, appears to be an essential tool in understanding the spatial distribution and temporal variation of the sedimentary contamination signature and thus beneficial for the management plan of the area.

Author contribution Anastasia Gkaragkouni: Conceptualization, Formal analysis, Investigation, Writing—Original Draft, Visualization, Writing—Review & Editing. Spyros Sergiou: Software, Formal analysis, Writing—Review & Editing, Visualization. Maria Geraga: Methodology, Investigation. Helen Papaefthymiou: Conceptualization, Validation. Dimitris Christodoulou: Software, Investigation, Visualization. George Papatheodorou: Conceptualization, Methodology, Supervision.

Declarations

Conflict of interest The authors declare no competing interests.

References

Ali, H., Khan, E., Ikram Ilahi, I. (2019). Environmental chemistry and ecotoxicology of hazardous heavy metals: Environmental persistence, toxicity, and bioaccumulation, *Journal of Chemistry,* ID 6730305 | https://doi.org/10.1155/2019/6730305

Angelidis, M., & Aloupi, M. (1995). Metals in sediments of Rhodes Harbour Greece. *Marine Pollution Bulletin, 31*, 273–276.

Angelidis, M., & Grimanis, A. P. (1987). Arsenic geochemistry in sediments near the Athens sewage outfall. *Marine Pollution Bulletin, 18*, 297–298.

Azimi, A., Azari, A., Rezakazemi, M., & Ansarpour, M. (2017). Removal of heavy metals from industrial wastewaters: A review. *ChemBioEng. Reviews, 4*, 37–59.

Barbieri, M. (2016). The importance of Enrichment Factor (EF) and Geoaccumulation Index (I_{geo}) to evaluate the soil contamination. *Journal of Geology & Geophysics, 5*, 237.

Bataillard, P., Grangeon, S., Quinn, P., Mosselmans, F., Lahfid, A., Wille, G., Joulian, C., & Battaglia-Brunet, F. (2014). Iron and arsenic speciation in marine sediments undergoing a resuspension event: The impact of biotic activity. *Journal of Soils and Sediments, 14*, 615–629.

Bhuiyan, M. K. A., Qureshi, S., Billah, M. M., Kammella, S., & V, Alam M.R., Ray, S., Monwar, M.M., & Hena, A. M. K., . (2018). Distribution of trace metals in channel sediment: A case study in South Atlantic Coast of Spain. *Water, Air, & Soil Pollution, 219*, 14.

Bi, S., Yang, Y., Xu, C., Zhang, Y., Zhang, X., & Zhang, X. (2017). Distribution of heavy metals and environmental assessment of surface sediment of typical estuaries in eastern China. *Marine Pollution Bulletin, 121*, 357–366.

Bincy, V. K., Dasog, G. S., Prasannakumar, B. H., Patil, C. R., & Hebbara, M. (2015). Chemical and microbial composition of municipal sewage water around Hubli-Dharwad in Karnataka. *Research Journal of Chemical and Environmental Sciences, 3*, 1–5.

Birch, G., & Taylor, S. (1999). Source of heavy metals in sediments of the Port Jackson estuary Australia. *The Science of the Total Environment, 227*, 123–138.

Boller, M. A., & Steiner, M. (2002). Diffuse emission and control of copper in urban surface runoff. *Water Science & Technology, 46*, 173–181.

Casado-Martnnez, C. M., Forja, M. J., & Delvalls, A. T. (2009). A multivariate assessment of sediment contamination in dredged materials from Spanish ports. *Journal of Hazardous Materials, 163*, 1353–1359.

Chaillou, G., Schafer, J., Anschutz, P., Lavaux, G., & Blanc, G. (2003). The behaviour of arsenic in muddy sediments of the Bay of Biscay (France). *Geochimica et Cosmochimica Acta, 67*, 2993–3003.

Chester, R., & Voutsinou, G. F. (1981). The initial assessment of trace metal pollution in coastal sediments. *Marine Pollution Bulletin, 12*, 84–91.

Christophoridis, C., Dedepsidis, D., & Fytianos, K. (2009). Occurrence and distribution of selected heavy metals in the surface sediments of Thermaikos Gulf, N Greece, Assessment Using Pollution Indicators. *Journal of Hazardous Materials, 168*, 1082–1091.

Christophoridis, C., Bourliva, A., Evgenakis, E., Papadopoulou, L., & Fytianos, K. (2017). Effects of anthropogenic activities on the levels of heavy metals in marine surface sediments of the Thessaloniki Bay, Northern Greece: Spatial distribution, sources and contamination assessment. *Microchemical Journal, 149*, 104001. https://doi.org/10.1016/j.microc.2019.104001

Clark, R. B. (2001). *Marine pollution* (p. 237). Oxford University Press.

Coxon, M. T., Odhiambo, K. B., & Giancarlo, C. L. (2016). The impact of urban expansion and agricultural legacies on trace metal accumulation in fluvial and lacustrine sediments of the lower Chesapeake Bay basin USA. *Science of the Total Environment, 569*, 402–414.

Crecelius, A. E. (1975). *The Geochemical Cycle of Arsenic in Lake Washington and Its Relation to Other Elements, 20*, 441–451.

Cukrov, N., Francisikovic-Bilinski, S., Hlaca, B., & Barisic, D. (2011). A recent history of metal accumulation in the sediments of Rijeka harbor Adriatic Sea, Croatia. *Marine Pollution Bulletin, 62*, 154–167.

Dasenakis, M., Ladakis, M., Karavoltsos, S., & Paraskevopoulou, V. (2015). *Chemical Oceanography* (pp. 978-960-603-234–9). National Technical University of Athens.

Davis, J. C. (1986). *Statistics and Data Analysis in Geology* (p. 647). Wiley.

Delshab, H., Farshchi, P., & Keshavarzi, B. (2017). Geochemical distribution, fractionation and contamination assessment of heavy metals in marine sediments of the Asaluyeh port Persian Gulf. *Marine Pollution Bulletin, 115*, 401–411.

Dixit, R., Wasiullah, D., Malaviya, K., Pandiyan, U., Singh, A., Sahu, R., Shukla, B., Singh, J., Rai, P., Sharma, H., Lade, D., & Paul, D. (2015). Bioremediation of heavy metals from soil and aquatic environment: An overview of principles and criteria of fundamental processes. *Sustainability, 7*, 2189–2212.

Fatoki, O. S., & Mathabatha, S. (2001). An assessment of heavy metal pollution in the East London and Port Elizabeth harbours. *Water S.A.* 27, 233–240

Folk, L.R., 1974. Petrology of sedimentary rocks, Austin, Texas

Galanopoulou, S., Vgenopoulos, A., & Conispoliatis, N. (2005). DDTs and other chlorinated organic pesticides and polychlorinated biphenyls pollution in the surface sediments of Keratsini harbour Saronikos Gulf, Greece. *Marine Pollution Bulletin, 50*, 520–525.

Galanopoulou, S., Vgenopoulos, A., & Conispoliatis, N. (2009). Anthropogenic heavy metal pollution in the surficial sediments of the Keratsini Harbour Saronikos Gulf Greece. *Water Air Soil Pollut, 202*, 121–130.

Gibert, O., Martinez-Llado, X., Marti, V., Diez, S., Romo, J., Bayona, M. J., & Pablo, J. (2009). Changes of heavy metal and PCB contents in surficial sediments of the Barcelona Harbour after the opening of a new entrance. *Water, Air, & Soil Pollution, 204*, 271–284.

Grimanis, P. A., Vassilaki-Grimani, M., & Griggs, B. G. (1977). Pollution studies of trace elements in sediments from the Upper Saronikos Gulf, Greece. *Journal of Radioanalytical Chemistry, 37*, 761–773.

Heap, J. M., Elliott, M., & Rheinallt, T. (1991). The marine disposal of sewage sludge. *Ocean and Shoreline Management, 16*, 291–312.

Hornberger, I. M., Luoma, N. S., Geen, A., Fuller, C., & Anima, R. (1999). Historical trends of metals in the sediments of San Francisco Bay California. *Marine Chemistry, 64*, 39–55.

Imdrie, J., & Purdy, E. G. (1962). Classification of modern Bahamian carbonate sediments, In: Classification of Carbonate Rocks, *Proceedings of the Symposium of American Association of Petroleum Geologists*, Memo 1, pp. 253–272.

Karageorgis, A. P., Sioulas, A., Krasakopoulou, E., Anagnostou, C. L., Hatiris, G. A., Kyriakidou, H., & Vasilopoulos, K., (2011). Geochemistry of surface sediments and heavy metal contamination assessment: Messolonghi lagoon complex, Greece. *Environmental Earth Sciences*.https://doi.org/10.1007/s12665-011-1136-3

Kersten, M., Garbe-Schonberg, C., Thomsen, S., Anagnostou, C., & Sioulas, A. (1997). Source apportionment of Pb pollution in the coastal waters of Elefsis Bay Greece. *Environmental Science & Technology, 31*, 1295–1301.

Kotzamanis, V., 1997. Athens, 1848 – 1995, Demographic emergency of a metropolis, Athens, Res. Society, 93, 3–30.

Lambrakis, N., Antonakos, A., & Panagopoulos, G. (2004). The use of multicomponent statistical analysis in hydrogeological environmental research. *Water Research, 38*, 1862–1872.

Lee, S. C., Li, X. D., Shi, W. Z., Cheung, S. C., & Thornton, I. (2006). Metal contamination in urban, suburban and country park soils of Hong Kong: A study based on GIS and multivariate statistics. *Science of the Total Environment, 356*, 45–61.

Leotsinidis, M., & Sazakli, E. (2008). Evaluating contamination of dredges and disposal criteria in Greek coastal areas. *Chemosphere, 72*, 811–818.

Lepland, A., Andersen, J. T., Lepland, A., Arp, H. P., Alve, E., Breedveld, G. D., & Rindby, A. (2010). Sedimentation and chronology of heavy metal pollution in Oslo harbor Norway. *Marine Pollution Bulletin, 60*(9), 1512–1522.

Li, X., Liu, E., Zhang, E., Lin, Q., Yu, Z., Nath, B., Yuan, H., Shen, J., 2020. Spatio-temporal variations of sedimentary metals in a large suburban lake in southwest China and the implications for anthropogenic processes, *Science of the Total Environment,* 707135650.

Long, E., MacDonald, D. D., Smith, S. L., & Calder, F. D. (1995). Incidence of adverse biological effects within ranges of chemical concentrations in marine and estuarine sediments. *Environmental Management, 19*, 81–97.

Maata, M., & Singh, S. (2008). Heavy metal pollution in Suva harbour sediments Fiji. *Environmental Chemistry Letters, 6*, 113–118.

Mara, D. (2003). *Domestic Wastewater Treatment in Developing Countries.* https://doi.org/10.4324/9781849771023

Moore, W. J., & Ramamoorthy, S. (1984). Heavy metals in natural waters: Applied Monitoring and Impact Assessment, Springer-Verlag; New York, 28- 246.

Moore, D. M., & Reynolds, R. C, Jr. (1989). *X-ray diffraction and the identification and analysis of clay minerals.* Oxford University Press (OUP), pp.332.

Mucci, A., Richard, L.-F., Lucotte, M., & Guignard, C. (2000). The differential geochemical behavior of arsenic and phosphorus in the water column and the sediments of the Saguenay Fjord Estuary Canada. *Aquatic Geochemistry, 6*, 293–324.

Muller, G. (1979). Schwermetalle in den Sedimenten des Rheins Veranderungen selt 1971. *Umschau, 79*, 778–783.

Muniz, P., Danulat, E., Yannicelli, B., García-Alonso, J., Medina, G., & Bícego, M. C. (2004). Assessment of contamination by heavy metals and petroleum hydrocarbons in sediments of Montevideo Harbour (Uruguay). *Environment International, 29*, 1019–1028.

Naifar, I., Pereira, F., Zmemla, R., Bouaziz, M., Elleuch, B., & Garcia, D. (2018). Spatial distribution and contamination assessment of heavy metals in marine sediments of the southern coast of Sfax Gabes Gulf, Tunisia. *Marine Pollution Bulletin, 131*, 53–62.

Oviatt, C., Quinn, J., Maughan, J., Ellis, T., Sullivan, B., Gearng, J., Gearing, P., Hunt, C., Sampou, P., Latimer, J. (1987). Fate and effects of sewage sludge in the coastal marine environment: A mesocosm experiment. *Marine Ecology – Progress Series*. 41:187–203

Owen, R. B., & Sandhu, N. (2000). Heavy metal accumulation and anthropogenic impacts on Tolo Harbour Hong Kong. *Marine Pollution Bulletin, 40*, 174–180.

Papaefthymiou, H., Papatheodorou, G., Christodoulou, D., Geraga, M., Moustakli, A., & Kapolos, J. (2010). Elemental concentrations in sediments of the Patras Harbour Greece, using INAA, ICP-MS and AAS. *Microchemical Journal, 96*, 269–276.

Papaefthymiou, H., Gkaragkouni, A., Papatheodorou, G., & Geraga, M. (2017). Radionuclide activities and elemental concentrations in sediments from a polluted marine environment (Saronikos Gulf-Greece). *Journal of Radioanalytical and Nuclear Chemistry, 314*, 1841–1852.

Papakostidis, G., Grimanis, P. A., & Zafiropoulos, D. (1975). Heavy metals in sediments from the Athens sewage outfall area. *Marine Pollution Bulletin, 6*, 136–139.

Papatheodorou, G., Hasiotis, T., & Ferentinos, G. (1993). Gas-charged sediments in the Aegean and Ionian Seas Greece. *Marine Geology, 112*, 171–184.

Papatheodorou, G., Lyberis, E., & Ferentinos, G. (1999). Use of factor analysis to study the distribution of metalliferous bauxitic tailings in the seabed of the Gulf of Corinth Greece. *Natural Resources Research, 8*, 277–286.

Papatheodorou, G., Hotos, G., Geraga, M., Avramidou, D., & Vorinakis, T. (2002). Heavy metal concentrations in sediments of Klisova lagoon (S.E. Mesolonghi-Aitolikon Lagoon complex) W Greece. *Fresenius Environmental Bulletin, 11*, 951–956.

Papatheodorou, G., Demopoulou, G., & Lambrakis, N. (2006). A long-term study of temporal hydrochemical data in a shallow lake using multivariate statistical techniques. *Ecological Modelling, 193*, 759–776.

Rezaee, Kh., Abdi, R. M., Saion, B. E., Naghavi, K., & Shafaei, A. M. (2011). Distribution of trace elements in the marine sediments along the South China Sea Malaysia. *Journal of Radioanalytical and Nuclear Chemistry, 287*, 733–740.

Romano, E., Ausili, A., Zharova, N., Magno, C. M., Pavoni, B., & Gabellini, M. (2004). Marine sediment contamination of an industrial site at Port of Bagnoli Gulf of Naples, Southern Italy. *Marine Pollution Bulletin, 49*, 487–495.

Salomons, W., & Forstner, U. (1984). *Metals in the Hydrocycle* (p. 349). Springer-Verlag, Berlin.

Samir, A. M., & El-Din, A. B. (2001). Benthic foraminifera assemblages and morphological abnormalities as pollution proxies in two Egyptian bays. *Marine Micropaleontology, 41*, 193–227.

Saxby, J. D. (1973). Diagenesis of metal-organic complexes in sediments: Formation of metal sulphides from cysteine complexes. *Chemical Geology, 12*, 241–288.

Sindermann, C. J. (2006). *Effects on living resources and humans*. FL, USA CRC Press.

Sprovieri, M., Feo, M. L., Prevedello, L., Manta, D. S., Sammartino, S., Tamburrino, S., & Marsella, E. (2007). Heavy metals, polycyclic aromatic hydrocarbons and polychlorinated biphenyls in surface sediments of the Naples harbor (southern Italy). *Chemosphere, 67*, 998–1009.

Stronkhorst, J., & Van Hattum, B. (2003). Contaminants of concern in Dutch marine harbor sediments. *Archives of Environmental Contamination and Toxicology, 45*, 306–316.

Tang, C. W., Ip, C. C., Zhang, G., Shin, P. K., Qian, P. Y., & Li, X. D. (2008). The spatial and temporal distribution of heavy metals in sediments of Victoria Harbour Hong Kong. *Marine Pollution Bulletin, 57*, 816–825.

Tessier, A. (1982). Particulate trace metal speciation in stream sediments and relationships with grain size: Implications for geochemical exploration. *Journal of Geochemical Exploration, 16*, 77–104.

Tham, T. T., Lap, B. Q., Mai, N. T., Trung, N. T., Thao, P. P., & Huong, N. T. L. (2021). Ecological risk assessment of heavy metals in sediments of Duyen Hai seaport area in Tra Vinh Province Vietnam. *Water, Air, & Soil Pollution, 232*, 49.

Theodorou, I. A., & Perissoratis, C. (1991). Environmental considerations for design of the Athens Sea Outfall Saronikos Gulf, Greece. *Environmental Geology and Water Sciences, 17*, 233–248.

Tomilson, D. L., Wilson, J. G., Harris, C. R., & Jeffrey, D. W. (1980). Problems in the assessment of heavy metal levels in estuaries and the formation of a pollution index. *Helgoländer Meeresuntersuchungen, 33*, 566–575.

Tranchina, L., Bellia, S., Brai, M., Hauser, B., Rizzo, S., & Bartolotta, A. (2004). Chemistry, mineralogy and radioactivity in *Posidonia oceanica* meadows from north-western Sicily. *Chemistry and Ecology, 20*, 203–214.

Tranchina, L., Basile, S., Brai, M., Caruso, A., Cosentino, C., & Micciche, S. (2008). Distribution of heavy metals in marine sediments of Palermo Gulf (Sicily, Italy). *Water Air and Soil Pollution, 191*, 245–256.

Valette-Silver, J. N. (1993). The use of sediment cores to reconstruct historical trends in contamination of estuarine and coastal sediments. *Estuaries and Coasts, 16*, 577–588.

Van den Hurk, P., Eertman, R. H. M., & Stronkhorst, J. (1997). Toxicity of harbour canal sediments before dredging and after off-shore disposal. *Marine Pollution Bulletin, 34*, 244–249.

Voudouris, K., Lambrakis, N., Papatheodorou, G., & Daskalaki, P. (1997). An application of factor analysis for the study of the hydro-geological conditions in Plio-Pleistocene aquifers of NW Achaia (NW Peloponnesus, Greece). *Mathematical Geology, 29*, 43–59.

Voudouris, P., Melfos, V., Moritz, R., Spry, P.G., Ortelli, M., Kartal, T. (2010). Molybdenite occurrences in Greece: Mineralogy, geochemistry and rhenium content. In Scientific Annals of the School of Geology AUTH, *Proceedings of the XIX Congress of the Carpathian-Balkan Geological Association*. 369–378.

Voutsinou-Taliadouri, F. (1981). Metal pollution in the Saronikos Gulf. *Marine Pollution Bulletin, 5*, 163–169.

Walkley, A. (1947). A critical examination of a rapid method for determining organic carbon in soils: Effect of variations in digestion conditions and of inorganic soil constituents. *Soil Science, 63*, 251–264.

Wang, X. S., Wang, S. J., Zhu, G. C., & Mao, Y. M. (2011). A statistical approach for assessing heavy metal contamination in near-shore marine sediment cores: A case study from the Yellow Sea, China. *International Journal of Environmental Studies, 68*, 73–82.

Wedepohl, H. K. (1969). *Handbook of Geochemistry*. Springer-Verlag.

Zago, C., Giblin, A. E., & Bergamasco, A. (2001). Changes in the metal content of surficial sediments of Boston Harbor since the cessation of sludge discharge. *Marine Environmental Research, 51*, 389–415.

Zhang, C., Yu, Z.-G., Zeng, G.-M., Jiang, M., Yang, Z.-Z., Cui, F., Zhu, M.-Y., Shen, L.-Q., & Hu, L. (2014). Effects of sediment geochemical properties on heavy metal bioavailability. *Environment International, 73*, 270–281. https://doi.org/10.1016/j.envint.2014.08.010